This is a repository copy of *Current-induced domain wall motion:Comparison of STT and SHE*.

Current-induced domain wall motion: comparison of STT and SHE

J. Chureemart[a], S.Sampan-a-pai[a], S.Boonchui[b], R.W.Chantrell[c], P.Chureemart[a,*]

[a] *Department of Physics, Mahasarakham University, Mahasarakham, 44150, Thailand*

[b] *Department of Physics, Kasetsart University, Bangkok, 10900, Thailand*

[c] *Department of Physics, University of York, York, YO10 5DD, United Kingdom*

Abstract

In this work, the current-induced domain wall (DW) motion driven by spin Hall effect (SHE) is theoretically investigated via an atomistic model. The SHE is taken into account in the atomistic model as a Slonczewski torque term. We first consider a bilayer system consisting of a ferromagnetic layer (FM) adjacent to a heavy metal (HM). To study the effect of spin Hall angle and FM thickness on DW motion in perpendicularly magnetized FM, an in-plane current is injected into HM. The results show that the critical current density, DW velocity and DW displacement strongly depend on the spin Hall angle and thickness of FM. To demonstrate the efficiency of SOT, we also study the DW motion driven by spin-transfer torque (STT) in a FM/NM/FM system by injecting a charge current perpendicularly to the plane of the structure. The DW velocity and DW displacement of two cases are compared. At the same current density, it is clearly observed that the DW in the presence of SOT is more easily moved with higher velocity and DW displacement. In addition, the critical current density of SHE driven case is smaller compared with spin torque case. To move the DW with the velocity of 100 m/s, the injected current density required for the STT case could be 10 times as high as the SHE case. The proposed model can be used to optimize all factors for spintronic device design with low power consumption, fast speed and high endurance such as the DW-based devices and the perpendicularly magnetized SOT-MRAM.

Keywords: Domain wall motion, Spin-transfer torque, Spin-Hall effect

1. Introduction

Domain wall (DW) motion in nanowires with in-plane magnetic anisotropy driven by injecting spin polarized current has been intensively studied over the past decade [1, 2, 3, 4, 5, 6, 7, 8] due to its possible applications in DW-based spintronics devices compatible with low power consumption, high speed operation and high density storage such as the racetrack memory and MRAM [9, 10]. DW motion is induced by spin torque arising from the s-d exchange interaction between the conduction electrons and the local magnetization within the DW. The spin torque contributed from the adiabatic and non-adiabatic torques is determined by the relative angle between the spin of the conduction electrons and local magnetization implying the disappearance of spin torque in collinear systems [7, 8]. DW motion tends to be easily initiated in narrow DW because of the strong interaction between the spin current and the local magnetization gradient within the DW giving rise to a large STT. Recently, materials with perpendicular magnetic anisotropy (PMA) originating from the interfacial anisotropy between a ferromagnetic transition metal and an insulator [11, 10, 12], for example CoFeB/MgO, have become of great interest owing to their high anisotropy resulting in narrow DW. It also has been reported that a DW in nanowire with PMA is more easily displaced with lower current density than that with in-plane anisotropy. STT effect seems to be more efficient in perpendicularly magnetized material since higher DW velocities are observed [13, 14]. However, STT becomes limited in a number of ways. The critical current density required to initiate DW motion in PMA nanowire is decreased, but the Joule heating still constrains the application of current-induced DW motion driven by STT.

The spin Hall effect (SHE) has been proposed as an alternative mechanism for fast current-induce DW mo-

---

*P. Chureemart, Email address: phanwadee.c@msu.ac.th

tion [15, 16, 17, 18, 19, 20]. Ryu et al. [21] and Emori et al. [22] experimentally demonstrated the enhancement of current-induced torque in a bilayer system, consisting of a heavy metal (such as Pt or Ta) and a ferromagnet. The mechanism behind the SHE can be described by injecting in-plane current into a nonmagnetic heavy metal in which the spin up and spin down electrons are scattered in opposite directions. This scattering results in pure spin current flowing into the ferromagnetic layer in the perpendicular direction to the injected electrical current. It can be another source of spin torque acting on the magnetization in the ferromagnet [22]. SHE offers a more efficient route to control magnetization since it evidently shows that SHE exhibits larger magnitude than the STT. It would be an essential step towards the magnetoelectric control of spintronic devices.

In this work, we firstly investigate the influence of SHE on DW motion in perpendicularly magnetized FM/HM structure by means of atomistic model. To observe the dynamic of magnetization in presence of SHE, the SHE is taken into account the atomistic model as the Slonczewski torque. We also study the effect of spin Hall angle and thickness of ferromagnet on the critical current density which is the minimum current density required to initiate DW motion. In addition, we demonstrate the efficiency of SHE by making a comparison with DW motion driven by STT in a trilayer system where the charge current is perpendicularly injected into the plane. These investigations show that SHE offers the possibility to manipulate the magnetization within DW by injecting in-plane current into the heavy metal adjacent to the ferromagnetic layer. This gives rise to increased efficiency of spin torque switching. The atomistic model including SHE can be used as the powerful tool to optimize all crucial parameters for SHE-based device design and it becomes increasingly important with further scaling of device dimensions especially for the application of CoFeB/MgO-based MTJ where the magnetic properties of interface and bulk are different [23, 24].

2. Model Description

In general, the spin-orbit torque field arising from both the Rashba and spin Hall effects. The former is phenomenon related to the interfacial spin-orbit coupling and the latter is the bulk effect depending on the thickness of the heavy metal [25]. In this work, we now consider the effect of the spin current arising from the SHE on the magnetization dynamics. The spin current leads to a spin-orbit torque due to SHE acting on the local magnetization which is qualitatively different from

the spin torque. To observe the magnetization dynamic in the presence of SHE, it can be represented as an additional spin torque in the LLG equation in the Slonczewski form as follows [26, 27, 28, 29, 30],

$$\frac{\partial \mathbf{S}}{\partial t} = -\gamma \mathbf{S} \times \mathbf{B}_{\text{eff}} + \alpha \mathbf{S} \times \frac{\partial \mathbf{S}}{\partial t} - \gamma B_{\text{SH}}[\mathbf{S} \times (\mathbf{S} \times \sigma)] \quad (1)$$

where $B_{\text{SH}} = \frac{\hbar \theta_{\text{SH}} j_e V}{2 e \mu_s t}$ is the spin Hall field, θ_{SH} is the spin Hall angle which is the ratio of the spin current density due to SHE and the electrical current density (j_e), t is the thickness of ferromagnetic layer and σ denotes SHE spin direction.

For the convenient integration, the above equation can be converted into the Landau-Lifshitz-Gilbert (LLG) form,

$$\begin{aligned}
\frac{\partial \mathbf{S}}{\partial t} &= -\frac{\gamma}{(1+\alpha^2)} \mathbf{S} \times \mathbf{B}_{\text{eff}} - \frac{\gamma \alpha}{(1+\alpha^2)} [\mathbf{S} \times (\mathbf{S} \times \mathbf{B}_{\text{eff}})] \\
&\quad + \frac{\gamma \alpha B_{\text{SH}}}{(1+\alpha^2)} (\mathbf{S} \times \sigma) - \frac{\gamma B_{\text{SH}}}{(1+\alpha^2)} [\mathbf{S} \times (\mathbf{S} \times \sigma)],
\end{aligned}$$
$$(2)$$

where $\mathbf{S}$ is the local normalized spin moment, γ is the absolute gyromagnetic ratio and α is the damping constant. The effective field, $\mathbf{B}_{\text{eff}}$, is the contribution of the exchange field, the anisotropy field, the external applied field and the demagnetizing field. Apart from the damped precessional motion arising from the effective field, the presence of the spin Hall effect in the last two terms in Eq. (2) leads to an additional torque acting on the local magnetization. This shows that the SHE can be another source of precessional and damping motion of the magnetization. Similar to the STT, the torque due to SHE can either increase or decrease the natural damping of effective field depending on the sign of spin Hall angle. The faster relaxation toward the direction of the effective field can be occurred in the case that the damping torque due to SHE is in the same direction as the natural damping.

The effective field acting on the local spin moment in Eq. (2) can be determined from a classical spin Hamiltonian representing the energies of the magnetic system. The spin Hamiltonian in Eq. (3) includes the contribution of the exchange energy, magnetic anisotropy energy, external applied field and the interfacial DMI energy [31, 27, 30] written as

$$\begin{aligned}
\mathcal{B} = &-\sum_{i<j} J_{ij} \mathbf{S}_i \cdot \mathbf{S}_j - k_{\text{u}} \sum_i (\mathbf{S}_i \cdot \mathbf{e})^2 - |\mu_s| \sum_i \mathbf{S}_i \cdot \mathbf{B}_{\text{app}} \\
&- D[S_z \nabla \cdot \mathbf{S}_i - (\mathbf{S}_i \cdot \nabla) S_z],
\end{aligned}$$
$$(3)$$

where J_{ij} is the nearest neighbor exchange integral between spin sites i and j, $\mathbf{S}_i$ is the local normalized spin

moment, $\mathbf{S}_j$ is the normalized spin moment of the neighboring atom at site j, k_u is the uniaxial anisotropy constant, $\mathbf{e}$ is the unit vector of the easy axis and $|\mu_s|$ is the magnitude of the spin moment and D is the DMI (Dzyaloshinskii-Moriya interaction) parameter.

In addition, the demagnetizing field can be taken into account in the model by adopting a micromagnetic discretization approach [31, 5] since its calculation is time consuming. The magnetic moment of each macrocell is determined by the summation of the atomic spins within the cell. The demagnetizing field of macrocell k containing spin i is given by

$$\mathbf{B}_{\mathrm{dip},k} = \frac{\mu_0}{4\pi} \sum_{l \neq k} \left[\frac{3(\mu_l \cdot \hat{\mathbf{r}}_{kl})\hat{\mathbf{r}}_{kl} - \mu_l}{|r_{kl}|^3} \right] - \frac{\mu_0}{3} \frac{\mu_k \hat{\mu}_k}{V} \quad (4)$$

and

$$\mu_l = \mu_s \sum_{i=1}^{n_{atom}} \mathbf{S}_i \quad (5)$$

where μ_l is the vector of the magnetic moment in the macrocell site l, μ_0 is the permeability of free space, V is the volume of the macrocell, r_{kl} is the distance and $\hat{\mathbf{r}}_{kl}$ the corresponding unit vector between macrocell sites k and l and n_{atom} is the number of atoms in each macrocell. It is worthwhile to note that the dipolar field with in each cell is taken as representative of all spins within the cell.

Consequently the effective local field which includes exchange, anisotropy, external fields, spin torque field, DMI field and the demagnetization contribution acting on the spin site i in the atomistic model is given by

$$\mathbf{B}_{\mathrm{eff},i} = -\frac{1}{|\mu_s|} \frac{\partial \mathcal{B}}{\partial \mathbf{S}_i} + \mathbf{B}_{\mathrm{dip},k}. \quad (6)$$

To investigate the dynamical magnetization behavior including the effect of the SHE, the local effective field from the above equation is substituted into Eq. (2) and the solution of the standard LLG equation is solved numerically by implementing the Heun integration scheme.

3. Results and discussion

In order to understand and compare the effect of STT and SHE on DW motion, we apply the proposed model to the bilayer system of FM/HM to study the effect of SHE. We have carried out a parametric investigation of the effects of the spin Hall angle and current density and the thickness dependence of DW motion. Subsequently, to show the efficiency of new path way of current-induced DW motion, we make a comparison of

the DW motion driven by SHE in the bilayer system with the STT in the trilayer system. Our findings are qualitatively consistent with experiment.

3.1. DW motion driven by SHE: parametric studies

We initially perform the simulations of current-induced DW motion driven by the SHE in the bilayer system consisting of a ferromagnet (FM) with perpendicular magnetic anisotropy (PMA) adjacent to the heavy metal (HM) as demonstrated in Fig. 1. The HM thickness is assumed to be infinite and the SHE is the major contribution to the SOT field [25]. We consider the ferromagnetic film with dimensions of $60 \times 30 \times 0.9 \, \text{nm}^3$. The magnetic properties of the ferromagnetic film (Co) used in this paper are as follows: a uniaxial anisotropy constant of $k_u = 6.69 \times 10^{-24} \text{J/atom}$ with the easy axis in z direction and the exchange integral of $6.06 \times 10^{-21} \text{J/link}$. The magnetization structure within DW can be obtained by means of the atomistic simulation by pinning the magnetization at the boundary of the structure in the easy axis direction, $\pm z$, to force the formation of a DW aligned in the xz plane. It is worth noting that the presence of PMA contribution from the interface is not considered explicitly.
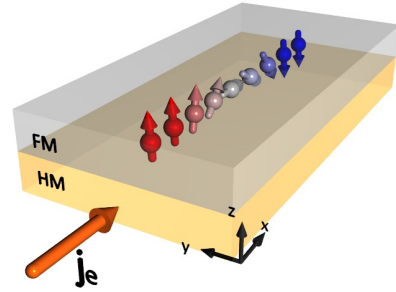

Figure 1: (Color online) Schematic illustration of the bilayer system of FM/HM: The arrows represent the direction of the magnetization within the DW in the ferromagnet.

The effect of SHE can be highlighted by performing atomistic model simulations in the absence of the contributions of STT and DMI. The spin current generated in HM via the spin-orbit interaction at the interface of FM/HM diffuses into the adjacent FM. We note that the SHE switching mechanism arises from the spin current flowing into the FM. This subsequently gives rise to the SHE acting on the magnetization. The magnitude of the SHE efficiency naturally depends on the spin current diffusing into the FM layer which is characterized by the spin Hall angle (θ_{SH}). Experimental studies report the important role of FM/HM interface to the intrinsic
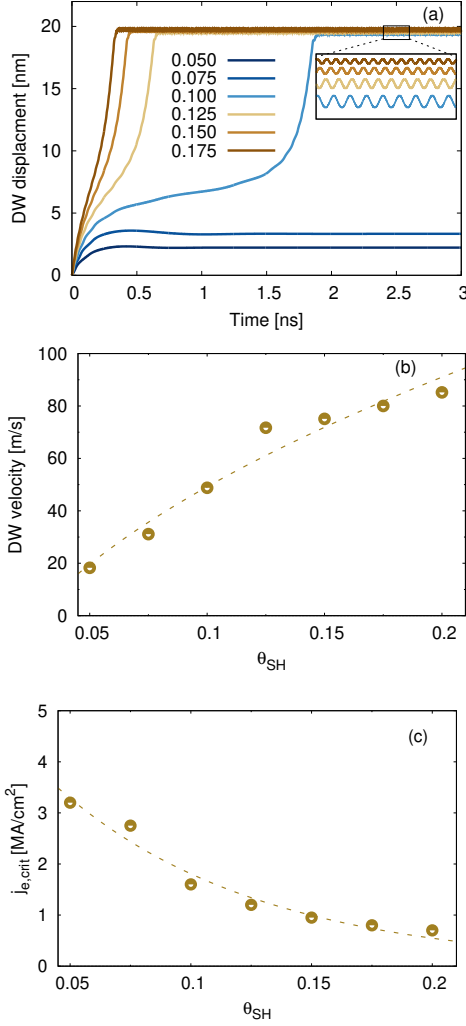
Figure 2: (Color online) DW motion in bilayer system of FM/NM with different spin Hall angles (a) time dependence of DW displacement (b) initial DW velocity and (c) the critical current density as a function of spin Hall angle

value of θ_{SH} [28, 29]. In this section, we therefore consider the influence of different interfaces of FM/HM on DW motion by introducing a charge current density of 5 MA/cm^2 into the heavy metal layer along the x direction and varying the value of θ_{SH} in the range of 0.05-0.2. It is worthwhile to note that the injected current density of 5 MA/cm^2 is greater than the critical current density to ensure that the DW motion is allowed.

DW motion driven by SHE is monitored by observing the displacement of the DW center from the initial position. Subsequently, the initial DW velocity can be calculated from the rate of change of the uniform DW displacement in the first 0.1 ns as demonstrated in Fig. 2 (a) and (b). We note that the finite size of the computational cell limits the DW displacement. The results show that the spin Hall angle representing the strength of the spin orbit coupling at the interface of FM/HM strongly affects the DW motion. For values of the spin Hall angle below 0.1, the DW has uniform translation to a finite DW displacement without any precession. For a high value of spin Hall angle, the DW can be easily moved with higher displacement and velocity after the introduction of spin current arising from the charge current injected into the HM layer.

In addition, we also observe the DW motion with oscillatory behavior around a finite DW displacement at a high frequency in the order of 200-300 GHz as shown in Fig. 2 (a) (inset). The oscillatory behavior of DW which can be applied for spin-torque oscillator is also observed in the previous studies [32, 33, 34]. This results from the out-of-plane component of magnetization due to the nonadiabatic torque of SHE. We also found the deformation of DW from the Néel wall to the Bloch wall. Interestingly, the appearance of DW displacement oscillation at high frequency of 300 GHz can be achieved by injecting current density of 5 MA/cm^2 which is much lower than the STT driven case in the previous study required a high current density up to 1000 MA/cm^2 [8]. This confirms that the SHE is more efficient to drive DW motion with larger velocities than the STT driven case. To improve the performance of the DW-based devices with high operating speed and low critical current density, this can be obtained by increasing spin Hall angle as clearly seen in Fig. 2 (c). The calculated critical current density in the range of 1 to 3 MA/cm^2 is in a good agreement with the experimental reports [35, 36]. This verifies the validity of proposed model.

The next case of interest is the effect of injected current density on DW motion by applying a charge current density ranging from 1 to 100 MA/cm^2 into the bilayer system of FM/HM with $\theta_{SH} = 0.15$ at zero temperature. It is important to note that the critical current density of this case is approximately 1 MA/cm^2. The effect of injected current density gives the similar results with that of spin Hall angle because the generated spin current diffusing into the ferromagnet is related with these two parameters. The high spin-polarized current can be obtained by using the material of HM with high spin Hall angle or injecting high charge current density. As a result in Fig. 3 (a), the DW motion can be initiated after the introduction of a current density above the critical value. For a high charge current density yielding high spin polarized current, the oscillatory behavior of the DW can be observed. The cause of the oscillation can be described that there is spin torque due to SHE acting on the magnetization within DW resulting in DW mo-
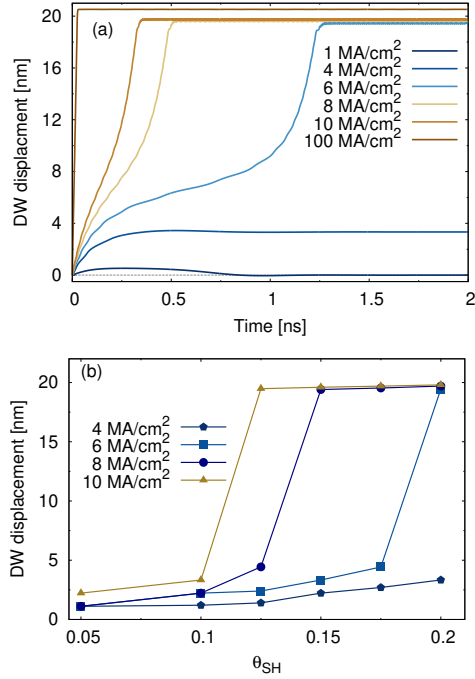
4

Figure 3: (Color online) (a) The time-dependent variation of the DW displacement for different current densities (b) DW displacement at equilibrium for different current densities and spin Hall angles
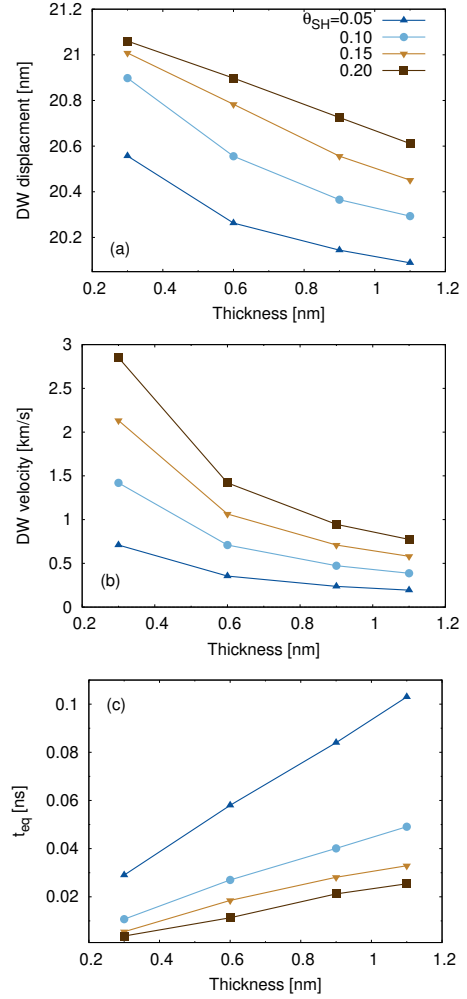
Figure 4: (Color online) Thickness dependence of (a) DW displacement, (b) DW velocity and (c) equilibration time for the SHE DW driven case with charge current density of 100 MA/cm^2 for different spin Hall angles

tion. Subsequently, the DW reaches and interacts with the strong pinning sites at the boundary. The frequency of the oscillation can be increased with increasing injected current density. However, the amplitude of the oscillation decreases and the equilibrium state without any precession can be appeared in the case of injecting very high current density. It is also found that the DW reaches the precessional steady state rapidly with high velocity over 400 m/s consistent with the previous reports [37]. Furthermore, the effect of current density and spin Hall angle on the DW displacement at the equilibrium are considered. As expected, increasing spin Hall angle and injected in-plane charge current density yielding higher transverse spin current in the adjacent ferromagnet results in the spin torque acting on the magnetization of ferromagnet and it consequently increases the DW displacement at equilibrium.

The magnitude of SHE depending on several parameters as expressed in the relation $B_{SH} = \hbar\theta_{SH}j_eV/(2e\mu_s t)$. We then investigate the FM thickness dependence of DW motion in HM/FM system with different spin Hall angles. Fig. 4 (a), (b) and (c) show the DW displacement, DW velocity and equilibration time as a function of FM thickness varied from 0.3 to 1.1 nm. The in-plane current density of 100 MA/cm^2 is in-

jected into the bilayer structure. The reduction of DW displacement and velocity can be observed when the thickness of FM is increased. This can be explained from the expression in Eq. (1) that the field arising from SHE is inversely proportional to the thickness of FM. This results in high SHE exerted on the magnetization within DW. In addition, for the thin film structure with high spin Hall angle, the high spin current can be generated and diffused into the ferromagnetic layer. The DW motion with high velocity and displacement can be achieved. Eventually, the DW can reach equilibrium rapidly which can be seen from the equilibration time.

3.2. Direct comparison: STT and SHE driven cases

For a better understanding of the efficiency of SHE in driving DW, we complete our study by performing additional investigation of DW motion driven by the STT in the Co/Cu/Co structure. In this work, we focus on the current perpendicular to plane (CPP) geometry instead of current in plane (CIP) geometry. This is due that a strong spin-dependent scattering in CPP geometry yields higher magnitude of STT. As shown in Fig. 5, the first and second FMs are regarded as the pinned layer (PL) and free layer (FL) respectively. The charge current is injected perpendicularly to the plane of the structure. To investigate the magnetization dynamic in the presence of STT, the effect of STT can be considered as the additional field arising from the s-d exchange interaction between the local magnetization and the spin accumulation into the effective field as shown in Eq. (7),

$$
\begin{aligned}
\frac{\partial \mathbf{S}}{\partial t} = &- \frac{\gamma}{(1+\alpha^2)} \mathbf{S} \times (\mathbf{B}_{\text{eff}} + J_{\text{sd}}\mathbf{m}) \\
&- \frac{\gamma\alpha}{(1+\alpha^2)} [\mathbf{S} \times (\mathbf{S} \times (\mathbf{B}_{\text{eff}} + J_{\text{sd}}\mathbf{m}))], \quad (7)
\end{aligned}
$$

where J_{sd} is the s-d exchange energy between electron spin and local spin moment and $\mathbf{m}$ is the spin accumulation.

The general solution of the spin accumulation in the basis coordinate system consists of the longitudinal ($\mathbf{m}_{\parallel}$) and transverse ($\mathbf{m}_{\perp}$) components which are parallel and perpendicular to the local magnetization given
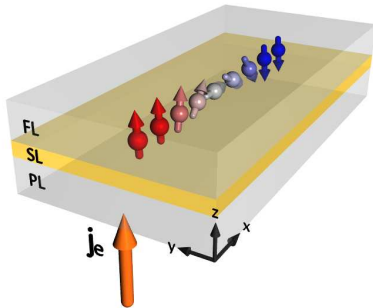

Figure 5: (Color online) The trilayer system consisting of two ferromagnetic layers separated by the nonmagnet (spacer layer): the tail-to-tail DW is formed in the xz plane of the free layer.
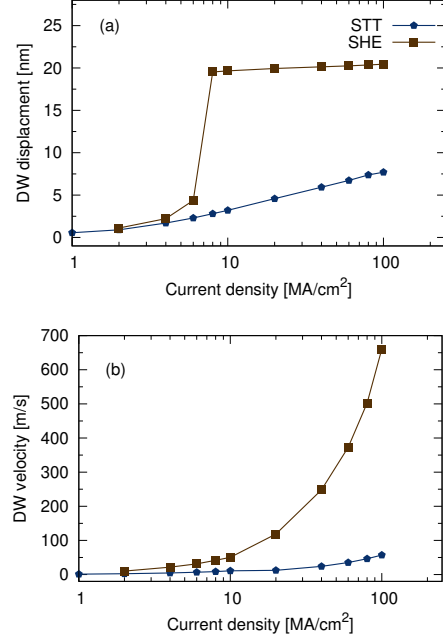

Figure 6: (Color online) (a) DW displacement and (b) velocity as a function of current density for the conventional STT and SHE driven cases

by [8, 38],

$$
\begin{aligned}
\mathbf{m}_{\parallel}(x) &= \left[m_{\parallel}(\infty) + \left[m_{\parallel}(0) - m_{\parallel}(\infty) \right] e^{-x/\lambda_{sdl}} \right] \hat{\mathbf{b}}_1 \\
\mathbf{m}_{\perp,2}(x) &= 2e^{-k_1 x} [u\cos(k_2 x) - v\sin(k_2 x)] \hat{\mathbf{b}}_2 \\
\mathbf{m}_{\perp,3}(x) &= 2e^{-k_1 x} [u\sin(k_2 x) + v\cos(k_2 x)] \hat{\mathbf{b}}_3,
\end{aligned}
$$

$$(8)$$

with

$$
(k_1 \pm i k_2) = \sqrt{\lambda_{\text{sf}}^{-2} \pm i\lambda_J^{-2}}.
$$

where $m_{\parallel}(\infty)$ is the spin accumulation at the equilibrium, the length scale λ_J is defined as $\lambda_J = \sqrt{2\hbar D_0/J}$ and λ_{sf} denotes the spin relaxation length. The coefficients $m_{\parallel}(0)$, u and v are constants which can be determined from the interface condition of the continuity of spin current.

The effect of current density on DW motion driven by the STT in a trilayer system and SHE in a bilayer system are investigated. We then make a direct comparison of DW displacement and velocity obtained from two cases. For the SHE driven case, we consider the HM/Co system with the spin Hall angle of 0.15. We perform the simulations by injecting charge current perpendicular to the plane for the STT driven case and in plane for the SHE driven case with the density from 1

6

to 100 MA/cm^2. The dynamic of the magnetization within DW in the presence of the SHE can be obtained by using Eq. (2) as mentioned previously and the atomistic model coupled with the spin accumulation model in Eq. (7) is used for the STT driven case. Interestingly, it is found that the critical current density of the SHE driven case is lower than that of the STT driven case. As a result demonstrated in Fig. 6, at the same current density the SHE driven case gives a higher value of DW velocity and displacement compared with STT driven case. The results show that the DW under the SHE can propagates faster with higher efficiency. Furthermore, to move the DW with the velocity of 100 m/s, the injected current density required for the STT case could be 10 times as high as the SHE case. This confirms that the SHE induced spin transfer torque promotes a fast-current induced DW motion. Our finding is consistent with previous report [20, 26] indicating that the DW motion driven by SHE can be observed for a Néel DW in perpendicularly magnetized strip. The investigation of current-induced DW motion driven by SHE proposes the new possibility to improve the performance of the next-generation DW-based SHE devices with a lower current density and higher efficiency. However, it is important to note that the efficiency of SHE for the application of magnetization reversal in MTJ could be different from the case of DW motion.

4. Conclusions

In summary, we theoretically study the current-induced DW motion in perpendicularly magnetized ferromagnet for two cases: the STT driven case and the SHE driven case. We perform the simulations for parametric studies by using the atomistic model. The results show that SHE provides higher efficiency of spin torque and a low current density to drive DW motion than the STT. The SHE is very promising to improve the performance of next-generation spintronic devices by using the appropriate materials with high spin Hall angle for HM/FM structure. To design spintronic device compatible with low power consumption, high speed operation and high density storage, the proposed model could be the useful tool to optimise important factors such as film thickness, spin hall angle and current density. It also provides a better understanding of the mechanisms governing the underlying physics behind the current induced DW motion driven by SHE.

References

[1] Z. Li, S. Zhang, Domain-wall dynamics driven by adiabatic spin-transfer torques, Phys. Rev. B 70 (2004) 024417.

[2] Z. Li, S. Zhang, Domain-wall dynamics and spin-wave excitations with spin-transfer torques, Phys. Rev. Lett. 92 (2004) 207203.

[3] R. P. Cowburn, Change of direction, Nature Materials 6 (2007) 255.

[4] S. S. P. Parkin, M. Hayashi, L. Thomas, Magnetic domain-wall racetrack memory, Science 320 (5873) (2008) 190–194.

[5] P. Chureemart, R. F. L. Evans, R. W. Chantrell, Dynamics of domain wall driven by spin-transfer torque, Phys. Rev. B 83 (2011) 184416.

[6] B. Beyersdorff, S. Hankemeier, S. Rößler, Y. Stark, G. Hoffmann, R. Frömter, H. P. Oepen, B. Krüger, Thermal effects in spin-torque assisted domain wall depinning, Phys. Rev. B 86 (2012) 184427.

[7] D. Claudio-Gonzalez, A. Thiaville, J. Miltat, Domain wall dynamics under nonlocal spin-transfer torque, Physical review letters 108 (22) (2012) 227208.

[8] P. Chureemart, R. F. L. Evans, I. D'Amico, R. W. Chantrell, Influence of uniaxial anisotropy on domain wall motion driven by spin torque, Phys. Rev. B 92 (2015) 054434.

[9] S. Tehrani, E. Chen, M. Durlam, M. DeHerrera, J. M. Slaughter, J. Shi, G. Kerszykowski, High density submicron magnetoresistive random access memory (invited), Journal of Applied Physics 85 (8) (1999) 5822–5827. ,

[10] S. Ikeda, K. Miura, H. Yamamoto, K. Mizunuma, H. Gan, M. Endo, S. Kanai, J. Hayakawa, F. Matsukura, H. Ohno, A perpendicular-anisotropy cofeb–mgo magnetic tunnel junction, Nature materials 9 (9) (2010) 721–724.

[11] S. Yakata, H. Kubota, Y. Suzuki, K. Yakushiji, A. Fukushima, S. Yuasa, K. Ando, Influence of perpendicular magnetic anisotropy on spin-transfer switching current in cofebmgocofeb magnetic tunnel junctions, Journal of Applied Physics 105 (7) (2009) 07D131. ,

[12] S. Fukami, T. Suzuki, Y. Nakatani, N. Ishiwata, M. Yamanouchi, S. Ikeda, N. Kasai, H. Ohno, Current-induced domain wall motion in perpendicularly magnetized cofeb nanowire, Applied Physics Letters 98 (8) (2011) 082504. ,

[13] T. A. Moore, I. M. Miron, G. Gaudin, G. Serret, S. Auffret, B. Rodmacq, A. Schuhl, S. Pizzini, J. Vogel, M. Bonfim, High domain wall velocities induced by current in ultrathin pt/co/alox wires with perpendicular magnetic anisotropy, Applied Physics Letters 93 (26) (2008) 262504. ,

[14] D. Chiba, M. Kawaguchi, S. Fukami, N. Ishiwata, K. Shimamura, K. Kobayashi, T. Ono, Electric-field control of magnetic domain-wall velocity in ultrathin cobalt with perpendicular magnetization, Nature Communications 3 (2012) 888 EP –, article.

[15] M. Dyakonov, V. Perel, Current-induced spin orientation of electrons in semiconductors, Physics Letters A 35 (6) (1971) 459 – 460.

[16] J. E. Hirsch, Spin hall effect, Phys. Rev. Lett. 83 (1999) 1834–1837.

[17] Y. K. Kato, R. C. Myers, A. C. Gossard, D. D. Awschalom, Observation of the spin hall effect in semiconductors, Science 306 (5703) (2004) 1910–1913. ,

[18] I. M. Miron, K. Garello, G. Gaudin, P.-J. Zermatten, M. V. Costache, S. Auffret, S. Bandiera, B. Rodmacq, A. Schuhl, P. Gambardella, Perpendicular switching of a single ferromagnetic layer induced by in-plane current injection, Nature 476 (7359) (2011) 189–193.

[19] L. Liu, C.-F. Pai, Y. Li, H. W. Tseng, D. C. Ralph, R. A. Buhrman, Spin-torque switching with the giant spin hall effect of tantalum, Science 336 (6081) (2012) 555–558. ,

[20] A. Thiaville, S. Rohart, É. Jué, V. Cros, A. Fert, Dynamics of dzyaloshinskii domain walls in ultrathin magnetic films, EPL (Europhysics Letters) 100 (5) (2012) 57002.

[21] K.-S. Ryu, L. Thomas, S.-H. Yang, S. Parkin, Chiral spin torque at magnetic domain walls, Nature nanotechnology 8 (7) (2013) 527.

[22] S. Emori, U. Bauer, S.-M. Ahn, E. Martinez, G. S. Beach, Current-driven dynamics of chiral ferromagnetic domain walls, Nature materials 12 (7) (2013) 611.

[23] H. Sato, P. Chureemart, F. Matsukura, R. W. Chantrell, H. Ohno, R. F. L. Evans, Temperature-dependent properties of cofeb/mgo thin films: Experiments versus simulations, Phys. Rev. B 98 (2018) 214428.

[24] S. Sampan-a pai, J. Chureemart, R. W. Chantrell, R. Chepulskyy, S. Wang, D. Apalkov, R. F. L. Evans, P. Chureemart, Temperature and thickness dependence of statistical fluctuations of the gilbert damping in Co-Fe-B/MgO bilayers, Phys. Rev. Applied 11 (2019) 044001.

[25] R. Ramaswamy, X. Qiu, T. Dutta, S. D. Pollard, H. Yang, Hf thickness dependence of spin-orbit torques in hf/cofeb/mgo heterostructures, Applied Physics Letters 108 (20) (2016) 202406. ,

[26] A. V. Khvalkovskiy, V. Cros, D. Apalkov, V. Nikitin, M. Krounbi, K. A. Zvezdin, A. Anane, J. Grollier, A. Fert, Matching domain-wall configuration and spin-orbit torques for efficient domain-wall motion, Phys. Rev. B 87 (2013) 020402.

[27] E. Martinez, S. Emori, N. Perez, L. Torres, G. S. D. Beach, Current-driven dynamics of dzyaloshinskii domain walls in the presence of in-plane fields: Full micromagnetic and one-dimensional analysis, Journal of Applied Physics 115 (21) (2014) 213909. ,

[28] W. Zhang, W. Han, X. Jiang, S.-H. Yang, S. S. P. Parkin, Role of transparency of platinumoeur"ferromagnet interfaces in determining the intrinsic magnitude of the spin hall effect, Nature Physics 11 (2015) 496 EP –.

[29] D. Bhowmik, M. E. Nowakowski, L. You, O. Lee, D. Keating, M. Wong, J. Bokor, S. Salahuddin, Deterministic domain wall motion orthogonal to current flow due to spin orbit torque, Scientific reports 5 (2015) 11823.

[30] S. A. Nasseri, S. Moretti, E. Martinez, C. Serpico, G. Durin, Collective coordinate models of domain wall motion in perpendicularly magnetized systems under the spin hall effect and longitudinal fields, Journal of Magnetism and Magnetic Materials 426 (2017) 195 – 201.

[31] R. F. L. Evans, W. J. Fan, P. Chureemart, T. A. Ostler, M. O. A. Ellis, R. W. Chantrell, Atomistic spin model simulations of magnetic nanomaterials, Journal of Physics: Condensed Matter 26 (10) (2014) 103202.

[32] A. Bisig, L. Heyne, O. Boulle, M. Kläui, Tunable steady-state domain wall oscillator with perpendicular magnetic anisotropy, Applied Physics Letters 95 (16) (2009) 162504. ,

[33] R. Sbiaa, R. W. Chantrell, Domain wall oscillations induced by spin torque in magnetic nanowires, Journal of Applied Physics 117 (5) (2015) 053907. ,

[34] R. Sbiaa, M. A. Bahri, S. Piramanayagam, Domain wall oscillation in magnetic nanowire with a geometrically confined region, Journal of Magnetism and Magnetic Materials 456 (2018) 324 – 328.

[35] L. Liu, C.-F. Pai, Y. Li, H. W. Tseng, D. C. Ralph, R. A. Buhrman, Spin-torque switching with the giant spin hall effect of tantalum, Science 336 (6081) (2012) 555–558. ,

[36] W. Chen, L. Qian, G. Xiao, Deterministic current induced magnetic switching without external field using giant spin hall effect of hth-w, Scientific Reports 8 (1) (2018) 8144.

[37] C. O. Avci, E. Rosenberg, M. Baumgartner, L. Beran, A. Quindeau, P. Gambardella, C. A. Ross, G. S. D. Beach, Fast switching and signature of efficient domain wall motion driven by spin-orbit torques in a perpendicular anisotropy magnetic insulator/pt bilayer, Applied Physics Letters 111 (7) (2017) 072406. ,

[38] N. Saenphum, J. Chureemart, R. Chantrell, P. Chureemart, Model of spin transport in noncollinear magnetic systems: Effect of diffuse interfaces, Journal of Magnetism and Magnetic Materials 484 (2019) 238 – 244.